

Probing New Physics in the Vector-like Lepton Model by Lepton Electric Dipole Moments

Koichi Hamaguchi^{a,b*}, Natsumi Nagata^{a†}, Genta Osaki^{a‡}, and Shih-Yen Tseng^{a§}

^a*Department of Physics, University of Tokyo, Bunkyo-ku, Tokyo 113-0033, Japan*

^b*Kavli IPMU (WPI), University of Tokyo, Kashiwa, Chiba 277-8583, Japan*

Abstract

We examine the lepton dipole moments in an extension of the Standard Model (SM), which contains vector-like leptons that couple only to the second-generation SM leptons. The model naturally leads to sizable contributions to the muon $g - 2$ and the muon electric dipole moment (EDM). One feature of this model is that a sizable electron EDM is also induced at the two-loop level due to the existence of new vector-like leptons in the loops. We find parameter regions that can explain the muon $g - 2$ anomaly and are also consistent with the experimental constraints coming from the electron EDM and the Higgs decay $h \rightarrow \mu^+ \mu^-$. The generated EDMs can be as large as $\mathcal{O}(10^{-22}) e \cdot \text{cm}$ for the muon and $\mathcal{O}(10^{-30}) e \cdot \text{cm}$ for the electron, respectively, which can be probed in future experiments for the EDM measurements.

*hama@hep-th.phys.s.u-tokyo.ac.jp

†natsumi@hep-th.phys.s.u-tokyo.ac.jp

‡osaki@hep-th.phys.s.u-tokyo.ac.jp

§shihyen@hep-th.phys.s.u-tokyo.ac.jp

1 Introduction

Last year, Fermilab published their first result [1] on the measurement of the muon anomalous magnetic moment

$$a_\mu \equiv \frac{g_\mu - 2}{2}, \quad (1)$$

which gives a value of

$$a_\mu(\text{exp}) = 116592061(41) \times 10^{-11}, \quad (2)$$

while the Standard Model (SM) prediction is [2]

$$a_\mu(\text{SM}) = 116591810(43) \times 10^{-11}. \quad (3)$$

There is a 4.2σ tension between the experiment and theory,

$$\Delta a_\mu = a_\mu(\text{exp}) - a_\mu(\text{SM}) = 251(59) \times 10^{-11}, \quad (4)$$

which may indicate the existence of physics beyond the Standard Model (BSM)¹.

Various new physics models have been proposed to explain this deviation. In general, these models contain hypothetical new particles and couplings, whose corresponding parameters are complex, and thus contain complex phases that break the CP symmetry. It is well-known that the flavor-conserving CP violation in the SM is very small, such that the induced particle electric dipole moments (EDMs) are vanishingly small. The non-zero SM contributions to lepton EDMs appear at the four-loop level and are thus strongly suppressed. For example, the electron EDM is estimated to be $|d_e^{\text{SM}}| \leq 10^{-38} e \cdot \text{cm}$ [6]. Since it is far below the sensitivity of the current experimental techniques, any observation of a particle EDM will be an unambiguous sign of the new physics beyond the SM.

Currently, the upper bound on the muon EDM is

$$|d_\mu| < 1.8 \times 10^{-19} e \cdot \text{cm} \quad (95\% \text{ C.L.}) \quad (5)$$

set by the Muon ($g - 2$) Collaboration at Brookhaven National Laboratory [7], which is about ten orders of magnitude weaker than the one on the electron EDM,

$$|d_e| < 1.1 \times 10^{-29} e \cdot \text{cm} \quad (90\% \text{ C.L.}) \quad (6)$$

set by the ACME Collaboration [8]. In order to improve the sensitivity on the muon EDM, there are several future experiments proposed to measure the muon EDM. For example, J-PARC Muon $g - 2$ /EDM experiment [9] and the one using the frozen-spin technique at the Paul Scherrer Institute (PSI) [10] will have sensitivities of $\sigma(d_\mu) \leq 1.5 \times 10^{-21} e \cdot \text{cm}$ and $\sigma(d_\mu) \leq 6 \times 10^{-23} e \cdot \text{cm}$, respectively.

¹The hadronic vacuum polarization (HVP) contribution to the muon $g - 2$ has been a challenge for theoretical calculations. The value obtained in the data-driven method, which is adopted in Ref. [2], is $a_\mu^{\text{HVP}} = 6845(40) \times 10^{-11}$. A discrepancy exists between this value and the lattice QCD calculations performed by the Budapest-Marseille-Wuppertal (BMW) group [3], which gives $a_{\mu, \text{BMW}}^{\text{HVP, LO}} = 7075(55) \times 10^{-11}$. This is 2.1σ larger than the recommended data-driven result. Naturally, the two values should be compatible with each other because they correspond to the same physical processes in the SM. However, the current situation is that there is a significant difference between the two approaches, and the reason is not yet clear. More intriguingly, recent results from other lattice QCD groups [4, 5] support the result obtained by the BMW group. For the time being, we simply fix on the value given in Eq. (3).

	ℓ_L	μ_R	H	$L_{L,R}$	$E_{L,R}$
$SU(3)_C$	1	1	1	1	1
$SU(2)_L$	2	1	2	2	1
$U(1)_Y$	$-\frac{1}{2}$	-1	$\frac{1}{2}$	$-\frac{1}{2}$	-1

Table 1: The quantum numbers of the SM and extra vector-like leptons in our model.

In this paper, we consider a model with extra vector-like leptons (VLLs) as a possible explanation of the muon $g - 2$ deviation, and investigate the EDMs of the muon and electron in the model. Models with VLLs have been discussed previously as solutions to the muon $g - 2$ anomaly [11–28]. See also Refs. [29–46] for the works that studied the muon EDMs in the models motivated by the muon $g - 2$ anomaly. We consider a simple extension to the SM with two vector-like leptons, one $SU(2)_L$ doublet and one $SU(2)_L$ singlet. We show that the model can naturally induce sizable EDMs of the muon and the electron at the one-loop and two-loop levels, respectively, in the parameter regions motivated by the muon $g - 2$; the predicted EDMs can be as large as $|d_\mu| \sim 10^{-22} e \cdot \text{cm}$ and $|d_e| \sim 10^{-30} e \cdot \text{cm}$, which are within the reach of the proposed EDM experiments. There are also researches discussing the indirect constraints on the muon EDM extracted from the EDM measurements of heavy atoms and molecules; for example, see Ref. [47].

This paper is structured as follows. In section 2, we describe the model used in the analysis. In section 3, we summarize the calculation of the one-loop contributions to the muon dipole moments. In section 4, the induced electron EDM in this model is discussed. The experimental constraints on this model are presented in section 5, and the results are given in section 6. Finally, we summarize the study in section 7.

2 Model

We consider an extension of the SM with one $SU(2)_L$ doublet (L) and one $SU(2)_L$ singlet (E) vector-like leptons. For simplicity, we consider the minimal scenario where the vector-like leptons couple only to the second-generation lepton, not to the first- and third-generation leptons.² Therefore, the electron and tau do not mix with extra vector-like leptons, and their masses totally originate from the Higgs Yukawa couplings. The quantum numbers of the fields necessary for the analysis are listed in Table 1, where ℓ_L and μ_R are the second-generation leptons in the SM and $L_{L,R}$ and $E_{L,R}$ denote the vector-like leptons, which respectively have the same quantum numbers as can be seen from the table. In the discussion below, our notation basically follows the one used in Ref. [13].

The components of the doublet fields are labeled as

$$\ell_L = \begin{pmatrix} \nu_\mu \\ \mu_L \end{pmatrix}, \quad L_{L,R} = \begin{pmatrix} L_{L,R}^0 \\ L_{L,R}^- \end{pmatrix}, \quad H = \frac{1}{\sqrt{2}} \begin{pmatrix} 0 \\ v + h \end{pmatrix}, \quad (7)$$

²Such kind of structure may be realized by imposing flavor symmetries on the model. We discuss a specific example in appendix B.

where $v = 246.22$ GeV is the vacuum expectation value of the Higgs field. In the rest of this paper, we denote the indices of muon and two vector-like leptons in the mass basis as 2, 4, 5, respectively, and for the muon, we use the symbol μ and 2 interchangeably.

Without loss of generality, we work in the basis where the Yukawa matrix of the leptons in the SM sector is already diagonal. The most relevant part of the Lagrangian is the Yukawa interactions among the muon and the vector-like leptons and the mass term of the vector-like leptons, which are given by³

$$\begin{aligned} \mathcal{L} \supset & -y_\mu \bar{\ell}_L \mu_R H - \lambda_E \bar{\ell}_L E_R H - \lambda_L \bar{L}_L \mu_R H - \lambda \bar{L}_L E_R H - \bar{\lambda} H^\dagger \bar{E}_L L_R \\ & - M_L \bar{L}_L L_R - M_E \bar{E}_L E_R + \text{h.c.} \end{aligned} \quad (8)$$

The parameters $y_\mu, \lambda_E, \lambda_L, \lambda, \bar{\lambda}, M_L$ and M_E are in general complex. However, most of the complex phases are not physical since they can be removed via field redefinitions. It turns out that in the model there are two independent complex phases

$$\phi_\lambda = \arg(y_\mu \lambda_L^* \lambda_E^* \lambda) \quad , \quad (9)$$

$$\phi_{\bar{\lambda}} = \arg(y_\mu \lambda_L^* \lambda_E^* M_L M_E \bar{\lambda}^*) \quad , \quad (10)$$

which are invariant under the phase rotation of the fields and therefore can serve as the sources of new CP violation. In this work, we take the two CP phases to be the phases of λ and $\bar{\lambda}$ and set the other parameters to be real.

After the Higgs field develops a vacuum expectation value, the leptons acquire masses and the mass matrix of charged leptons is given by

$$\bar{f}_L M f_R = (\bar{\mu}_L, \bar{L}_L^-, \bar{E}_L) \begin{pmatrix} y_\mu v/\sqrt{2} & 0 & \lambda_E v/\sqrt{2} \\ \lambda_L v/\sqrt{2} & M_L & \lambda v/\sqrt{2} \\ 0 & \bar{\lambda} v/\sqrt{2} & M_E \end{pmatrix} \begin{pmatrix} \mu_R \\ L_R^- \\ E_R \end{pmatrix}, \quad (11)$$

where the leptons in the flavor eigenbasis are denoted collectively as $f_L = (\mu_L, L_L^-, E_L)^T$ and $f_R = (\mu_R, L_R^-, E_R)^T$.

We can diagonalize the mass matrix in Eq. (11) by a bi-unitary transformation with two unitary matrices U_L and U_R :

$$U_L^\dagger \begin{pmatrix} y_\mu v & 0 & \lambda_E v \\ \lambda_L v & M_L & \lambda v \\ 0 & \bar{\lambda} v & M_E \end{pmatrix} U_R = \begin{pmatrix} m_2 & 0 & 0 \\ 0 & m_4 & 0 \\ 0 & 0 & m_5 \end{pmatrix}, \quad (12)$$

where the eigenmass m_2 is set to be the mass of muon, $m_2 = m_\mu$, and the mass ordering is fixed as $m_2 < m_4 < m_5$. We also note that the mass of the neutral component of the doublet L , $L^0 \equiv \nu_4$, solely originates from the mass term $-M_L \bar{L}_L L_R$ and hence its mass is determined by the value of M_L .

³In general, the other mass terms $M'_L \bar{\ell}_L L_R$ and $M'_R \bar{E}_L \mu_R$ are also allowed, but they can be removed by field redefinitions.

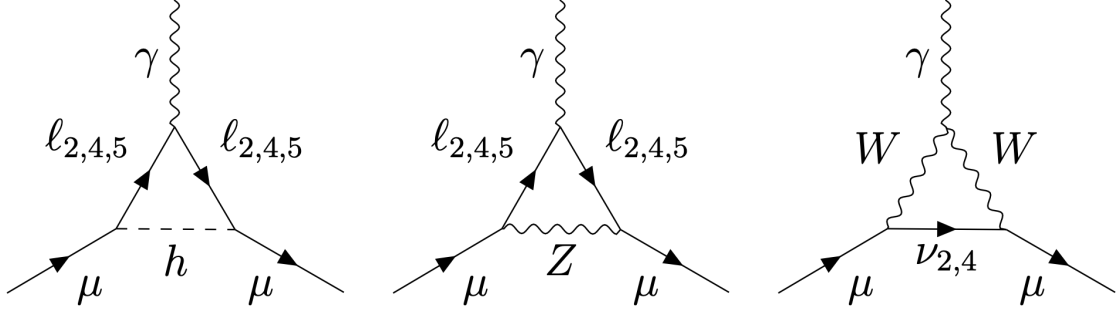


Figure 1: One-loop contributions to the muon dipole moments. $\ell_{2,4,5}$ are the muon and two vector-like leptons in the mass basis, while $\nu_{2,4}$ are the muon neutrino and the heavy neutrino in the vector-like doublet, respectively.

3 Muon dipole moments

In this section, we summarize the one-loop contributions to the dipole moments of the muon, which are induced by the diagrams of the Higgs, Z boson and W boson mediations, as shown in Fig. 1. For the relevant interactions, see appendix A.

3.1 Higgs boson mediation

The contributions to the muon dipole moments from the Higgs boson mediation are given by

$$\Delta a_\mu^h = \frac{m_\mu}{8\pi^2 m_h^2} \sum_{i=2,4,5} \left[(|\lambda_{i2}|^2 + |\lambda_{2i}|^2) m_\mu f_h(r_i) + \text{Re}(\lambda_{i2}\lambda_{2i}) m_i g_h(r_i) \right] - a_\mu^{h,\text{SM}}, \quad (13)$$

$$d_\mu^h = -\frac{e}{16\pi^2 m_h^2} \sum_{i=2,4,5} \text{Im}(\lambda_{i2}\lambda_{2i}) m_i g_h(r_i), \quad (14)$$

where $a_\mu^{h,\text{SM}}$ is the SM contribution from the diagram with muons in the loop. The loop functions are

$$g_h(r_i) = -\frac{r_i^2 - 4r_i + 3 + 2\ln(r_i)}{2(1-r_i)^3}, \quad (15)$$

$$f_h(r_i) = \frac{r_i^3 - 6r_i^2 + 3r_i + 2 + 6r_i \ln(r_i)}{12(1-r_i)^4}, \quad (16)$$

with $r_i = m_i^2/m_h^2$ and $i = 2, 4, 5$.

3.2 Z boson mediation

The contributions to the muon dipole moments from the Z boson mediation are given by

$$\Delta a_\mu^Z = \frac{m_\mu}{8\pi^2 m_Z^2} \sum_{i=2,4,5} \left\{ \left[|(g_L^Z)_{i2}|^2 + |(g_R^Z)_{i2}|^2 \right] m_\mu f_Z(r_i) + \text{Re} \left[(g_L^Z)_{i2} (g_R^{Z*})_{i2} \right] m_i g_Z(r_i) \right\} - a_\mu^{Z,\text{SM}}, \quad (17)$$

$$d_\mu^Z = \frac{e}{16\pi^2 m_Z^2} \sum_{i=2,4,5} \text{Im} \left[(g_L^Z)_{i2} (g_R^{Z*})_{i2} \right] m_i g_Z(r_i), \quad (18)$$

where $a_\mu^{Z,\text{SM}}$ is the SM contribution from the diagram with muons in the loop. The loop functions are then given by

$$g_Z(r_i) = -\frac{r_i^3 + 3r_i - 4 - 6r_i \ln(r_i)}{2(1 - r_i)^3}, \quad (19)$$

$$f_Z(r_i) = -\frac{5r_i^4 - 14r_i^3 + 39r_i^2 - 38r_i + 8 - 18r_i^2 \ln(r_i)}{12(1 - r_i)^4}, \quad (20)$$

with $r_i = m_i^2/m_Z^2$ and $i = 2, 4, 5$.

3.3 W boson mediation

The contributions to the muon dipole moments from the W boson mediation are given by

$$\Delta a_\mu^W = \frac{m_\mu}{8\pi^2 m_W^2} \left\{ \sum_{i=2,4} \left[|(g_L^W)_{i2}|^2 + |(g_R^W)_{i2}|^2 \right] m_\mu f_W(r_i) + \text{Re} \left[(g_L^W)_{42} (g_R^{W*})_{42} \right] M_L g_W(r_4) \right\} - a_\mu^{W,\text{SM}}, \quad (21)$$

$$d_\mu^W = \frac{e}{16\pi^2 m_W^2} \text{Im} \left[(g_L^W)_{42} (g_R^{W*})_{42} \right] M_L g_W(r_4), \quad (22)$$

where $a_\mu^{W,\text{SM}}$ is the SM contribution from the diagram with muon neutrino in the loop. The loop functions are given by

$$g_W(r_i) = \frac{r_i^3 - 12r_i^2 + 15r_i - 4 + 6r_i^2 \ln(r_i)}{2(1 - r_i)^3}, \quad (23)$$

$$f_W(r_i) = \frac{4r_i^4 - 49r_i^3 + 78r_i^2 - 43r_i + 10 + 18r_i^3 \ln(r_i)}{12(1 - r_i)^4}, \quad (24)$$

where $r_2 = m_{\nu_\mu}^2/m_W^2$ assuming $m_{\nu_\mu} \simeq 0$, and $r_4 = M_L^2/m_W^2$.

4 Electron EDM

In this model, the mixings among the muon and the extra vector-like leptons also contribute to the electron EDM. These contributions appear in the internal lepton loop of the two-loop Barr-Zee diagrams [48] shown in Fig. 2, where all possible combinations of muon and vector-like leptons contribute to the inner loop, as shown in Fig. 3.

To obtain the value of the electron EDM, let us first discuss the left diagram in Fig. 2. The first step is to extract the effective vertex $\Gamma_{hV\gamma}^{\mu\nu}$ from the inner loop. By the gauge invariance of the on-shell photon, $q_\mu \Gamma^{\mu\nu} = 0$, the effective vertex must have the form of [49]

$$\Gamma_{hV\gamma}^{\mu\nu,ij}(q, k) = \int_0^1 dx \frac{eQ}{4\pi^2 D^{ij}} \left[c_E^{Vij} (q^\nu k^\mu - q \cdot k g^{\mu\nu}) + i c_O^{Vij} \epsilon^{\mu\nu\alpha\beta} q_\alpha k_\beta \right], \quad (25)$$

where $V = \gamma, Z$, and Q is the charge of the lepton coupled to the external photon which is -1 for all cases considered here. The coefficients c_E^{Vij} , c_O^{Vij} , and the Δ^{ij} in the denominator

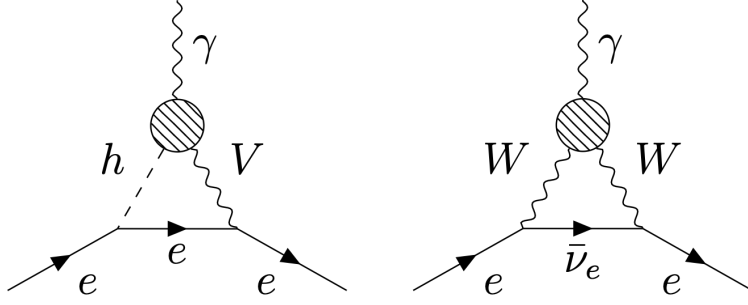


Figure 2: Contributions to the electron EDM from the Barr-Zee diagram induced by the vector-like leptons.

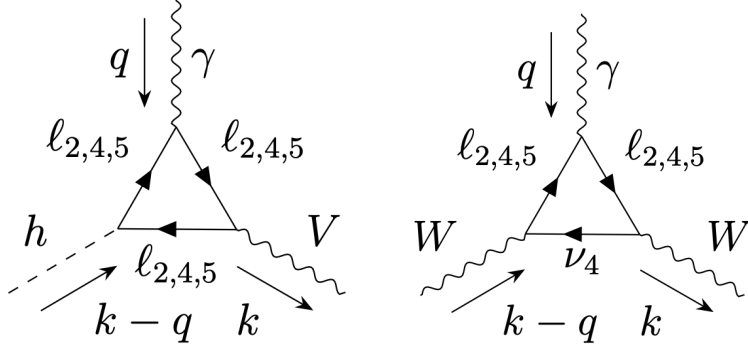


Figure 3: The inner loop inside the blob of Fig. 2.

are given by

$$c_E^{Vij} = m_i x^2 (1-x) (g_s^{ij*} g_v^{Vij} + g_p^{ij*} g_a^{Vij}) + m_j (1-x)^3 (g_s^{ij*} g_v^{Vij} - g_p^{ij*} g_a^{Vij}), \quad (26)$$

$$c_O^{Vij} = -m_i x (1-x) (g_s^{ij*} g_a^{Vij} + g_p^{ij*} g_v^{Vij}) + m_j (1-x)^2 (g_s^{ij*} g_a^{Vij} - g_p^{ij*} g_v^{Vij}), \quad (27)$$

$$D^{ij} = x(1-x)k^2 - xm_i^2 - (1-x)m_j^2. \quad (28)$$

Here, $i, j = 2, 4, 5$, and g_s, g_p, g_v^V, g_a^V are the couplings of scalar, pseudoscalar, vector, and axial-vector types, respectively.⁴ The particle j is defined as the one who interacts with the external photon, accompanied by particle i in the inner loop of the Barr-Zee diagram. The expression of the electron EDM from the $hV\gamma$ diagrams is given by

$$d_e^{hV\gamma} = \frac{eg_v^{Vee} g_s^{ee}}{32\pi^4} \sum_{i,j=2,4,5} \int_0^1 dx \text{Im}(c_O^{Vij}) I_{hV}^{ij}, \quad (29)$$

where g_v^{Vee} and g_s^{ee} are the SM couplings of the electron to vector bosons, $V = \gamma, Z$, and Higgs boson⁴. The momentum integration over k in the outer loop, I_{hV}^{ij} , is given by

$$I_{hV}^{ij} = \frac{1}{m_h^2} \left[F\left(x, \frac{m_V^2}{m_h^2}, \frac{\Delta_{ij}}{m_h^2}\right) - F\left(x, \frac{m_V^2}{m_h^2}, \frac{\Delta_{ij}}{m_V^2}\right) \right], \quad (30)$$

where

$$F(x, y, z) = \frac{1}{(1-y)[z-x(1-x)]} \ln \frac{z}{x(1-x)}, \quad (31)$$

$$\Delta_{ij} = xm_i^2 + (1-x)m_j^2. \quad (32)$$

⁴ The details of interaction couplings can be found in appendix A.

Another class of diagrams is the ones with two W bosons as shown in the right diagram of Fig. 2. In this case, the contribution to the electron EDM originates from the interaction of the heavy neutrino ν_4 with the charged leptons, and is given by

$$d_e^{WW\gamma} = \frac{eg^2}{256\pi^4} \sum_{i=2,4,5} \frac{m_e m_i M_L}{m_W^2} \text{Im} \left[(g_L^W)_{4i} (g_R^{W*})_{4i} \right] \int_0^1 dx I_{WW}^{4i}, \quad (33)$$

where

$$I_{WW}^{4i} = \frac{(1-x)}{-x(1-x)m_W^2 + (1-x)m_i^2 + xM_L^2} \ln \frac{(1-x)m_i^2 + xM_L^2}{x(1-x)m_W^2}. \quad (34)$$

5 Constraints

In this section, we discuss the constraints on the model of vector-like leptons coming from the precision electroweak measurements, the electron EDM, the Higgs decay $h \rightarrow \mu^+ \mu^-$, and the collider constraints on the heavy charged leptons.

5.1 Precision electroweak measurements

Since the muon and the muon neutrino mix with extra vector-like leptons in this model, the gauge couplings in the mass basis are modified (for details, see appendix A). Therefore, several electroweak observables are affected correspondingly, such as the muon lifetime, decay asymmetries involving muons, partial widths of W and Z bosons, etc. These constraints have been considered in the previous analysis [11, 26] and can be translated into upper bounds of the couplings λ_L and λ_E given by

$$\frac{\lambda_L v}{\sqrt{2}M_L} \lesssim 0.04, \quad \frac{\lambda_E v}{\sqrt{2}M_E} \lesssim 0.03. \quad (35)$$

5.2 $h \rightarrow \mu^+ \mu^-$

Since the Yukawa coupling of the muon is also modified from its SM value, the deviation from the SM prediction is expected in the decay channel of the Higgs boson to a muon pair, $h \rightarrow \mu^+ \mu^-$. In the latest search of this Higgs decay channel, the CMS group found the first evidence of the Higgs-to-dimuon decay channel [50] with a significance of three standard deviations. Currently, the branching fraction of $h \rightarrow \mu^+ \mu^-$ is constrained to be within the range $0.8 \times 10^{-4} < \mathcal{B}(h \rightarrow \mu^+ \mu^-) < 4.5 \times 10^{-4}$ at 95% confidence level. This can be transformed into

$$0.37 < R(h \rightarrow \mu^+ \mu^-) \equiv \frac{\Gamma(h \rightarrow \mu^+ \mu^-)}{\Gamma(h \rightarrow \mu^+ \mu^-)_{\text{SM}}} < 2.1, \quad (36)$$

where we have used $\Gamma(h \rightarrow \mu^+ \mu^-)_{\text{SM}} = 2.16 \times 10^{-4}$ [51] for $m_H = 125.25$ GeV [52]. In our setup, the ratio is given by $R(h \rightarrow \mu^+ \mu^-) = |\lambda_{22}|^2 / (m_\mu/v)^2$.

5.3 Electron EDM

The latest measurement of the electron EDM is performed by the ACME collaboration [8], which measured the precession of the electron spin in a superposition of the quantum states of an electron inside a strong intramolecular electric field. The group obtained an upper limit on the value of the electron EDM,

$$|d_e| < 1.1 \times 10^{-29} \text{ e} \cdot \text{cm} \quad (37)$$

at 90% confidence level. We note that in obtaining the above limit, possible contributions to the spin precession frequency from the CP -odd electron-nucleon scalar coupling are set to zero. In the case of the model of vector-like leptons, such kinds of coupling exist as higher-order quantum effects and, therefore, can be safely ignored in our analysis.⁵

5.4 Direct search of heavy leptons

The extra vector-like leptons decay via charged or neutral weak currents through the mixing with the SM second generation leptons. The tree-level decay modes include $\ell_i \rightarrow \ell_j + Z/h$, and $\ell_i \rightarrow \nu_j + W$, with $i > j$. However, there are not so many experimental searches concentrating on vector-like leptons compared to the searches on vector-like quarks.

The LEP experiment searched for such kinds of decays and set a lower bound on the mass of these new leptons [53]. The lower bound was set to be around 100 GeV. Recently, the CMS group reported the lower bound on the mass of vector-like leptons coupled to the third generation of SM lepton, τ [54]. The doublet type is constrained to be heavier than 1045 GeV, and for the singlet type, the mass range 125–150 GeV is excluded. Expecting that the constraints on the vector-like leptons coupled to the muons are comparable, in this study, we assume that the vector-like leptons have masses of $\mathcal{O}(1)$ TeV.

6 Results

In this section, we show the results of our analysis on the model of vector-like leptons. We randomly choose the sampling points and scan over the parameters in the model with the ranges of parameters listed in Table 2. We note that the masses of the vector-like leptons are chosen to be at the TeV scale in this analysis so that the constraints from the direct search of heavy leptons are avoided. The muon Yukawa coupling y_μ is solved for the correct muon mass with all other 8 parameters fixed randomly in the range indicated by Table 2. We note that in solving the Yukawa coupling, it can be written in the form of a quadratic equation, therefore there are in general two solutions of Yukawa coupling for each randomly chosen parameter set. We include both of them in the result.

⁵The size of these higher-order effects can be estimated from the results in Ref. [47], where the contribution of the muon EDM to the electron EDM d_e and the CP -odd electron-nucleon coupling C_S is evaluated. This is expressed in terms of the equivalent electron EDM, d_e^{equiv} , a linear combination of d_e and C_S that is constrained by experiments: $d_e^{\text{equiv}} \simeq 5.8 \times 10^{-10} d_\mu$. As we see in the subsequent section, in our model we have $|d_\mu| \lesssim 1.5 \times 10^{-22} \text{ e} \cdot \text{cm}$, and thus the size of the equivalent electron EDM induced radiatively by the muon EDM is $\lesssim 8.7 \times 10^{-32} \text{ e} \cdot \text{cm}$, which is smaller than the Barr-Zee contribution for most of the parameter points shown in Fig. 5.

Parameter	Value
M_L, M_E	1 – 5 TeV
$ \lambda_L , \lambda_E $	\leq EW constraints in Eq. (35)
$ \lambda , \bar{\lambda} $	0 – 1
$\phi_\lambda, \phi_{\bar{\lambda}}$	0 – 2π
y_μ	solved for the correct m_μ

Table 2: Ranges of parameters randomly chosen for the sampling points. Around 4×10^5 sampling points for the results are shown in the scattering plots.

In the left plot of Fig. 4, the correlation between the muon $g - 2$ and the muon EDM is shown. The horizontal red line and the (light) red bands correspond to the central value and (2σ) 1σ regions of the observed muon $g - 2$ in the experiment, respectively. The gray dots are the ones excluded by the $h \rightarrow \mu^+\mu^-$ constraint. After this selection, we further exclude the sampling points that predict the electron EDM to be too large and exceed the current upper bound given in Eq. (37). These are represented by the blue dots. The black dots are the sampling points that satisfy both the constraints from $h \rightarrow \mu^+\mu^-$ and electron EDM. We can see that there are predictions consistent with the observed muon $g - 2$, and the largest muon EDM is around $|d_\mu| \simeq 1.5 \times 10^{-22} e \cdot \text{cm}$. The PSI experiment [10] can examine some regions of the parameters, and its sensitivity to the muon EDM is shown by the vertical dotted line. In this result, we confirm the elliptical correlation between muon $g - 2$ and muon EDM obtained from the EFT approach [46].

In the right plot of Fig. 4, the correlation between the muon $g - 2$ and the electron EDM is shown. The gray dots show the sampling points excluded by the $h \rightarrow \mu^+\mu^-$ constraint, and the region with the blue band is excluded by the current limit on the electron EDM from the ACME experiment. From the plot, we see that most of the sampling points that are consistent with both the $h \rightarrow \mu^+\mu^-$ and muon $g - 2$ predict $|d_e| \gtrsim 10^{-32} e \cdot \text{cm}$. The vertical dashed line, $|d_e| = 10^{-30} e \cdot \text{cm}$, indicates a representative sensitivity of near future experiments. The next-generation ACME experiment (ACME III) is expected to improve the current sensitivity by an order of magnitude [55], and there are also proposals to improve the sensitivity by several orders of magnitude in the next 10-20 years [56].

In Fig. 5, we show the correlation between the muon and the electron EDMs. Again, we first excluded the sampling points that do not satisfy the $h \rightarrow \mu^+\mu^-$ constraint. These are the gray dots in the figure. The remaining sampling points are categorized into two classes, with the (dark) red dots representing the points satisfying the (1σ) 2σ region of the muon $g - 2$, respectively. The horizontal blue band is the constraint from the ACME experiment for the electron EDM measurement, and the prospects of the future muon/electron EDM experiments are also given in the plot. We find that these proposed experiments can investigate a significant fraction of the parameter space of this model, as they can exclude most of the available sampling points in the figure if no signals of EDMs are discovered. Furthermore, all of the allowed parameter space in Fig. 5 can be covered by the electron EDM experiments offering sensitivities better than the current value by several orders of magnitude [56].

Finally, we show the dependence of the muon and electron EDMs on the two CP -

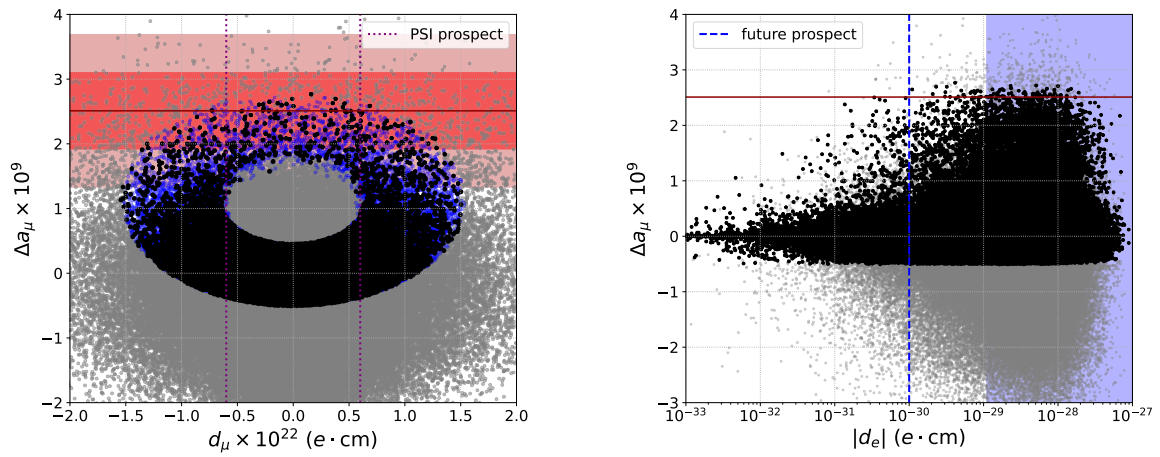


Figure 4: The correlations of muon $g - 2$ with muon EDM (left plot) and electron EDM (right plot). The horizontal red line and (light) red bands correspond to the central value and (2σ) 1σ regions of the observed muon $g - 2$, respectively. The $h \rightarrow \mu^+\mu^-$ constraint is first applied in both plots and the sampling points which do not satisfy it are shown as the gray dots. In the left plot, we also show the sampling points further excluded by the electron EDM constraint in blue. The black dots are the points that satisfy both the constraints from $h \rightarrow \mu^+\mu^-$ and electron EDM. The vertical dotted line represents the PSI experiment. In the right plot, the blue band shows the constraint from electron EDM measurement and the vertical dashed line indicates the prospect of the near-future electron EDM experiments.

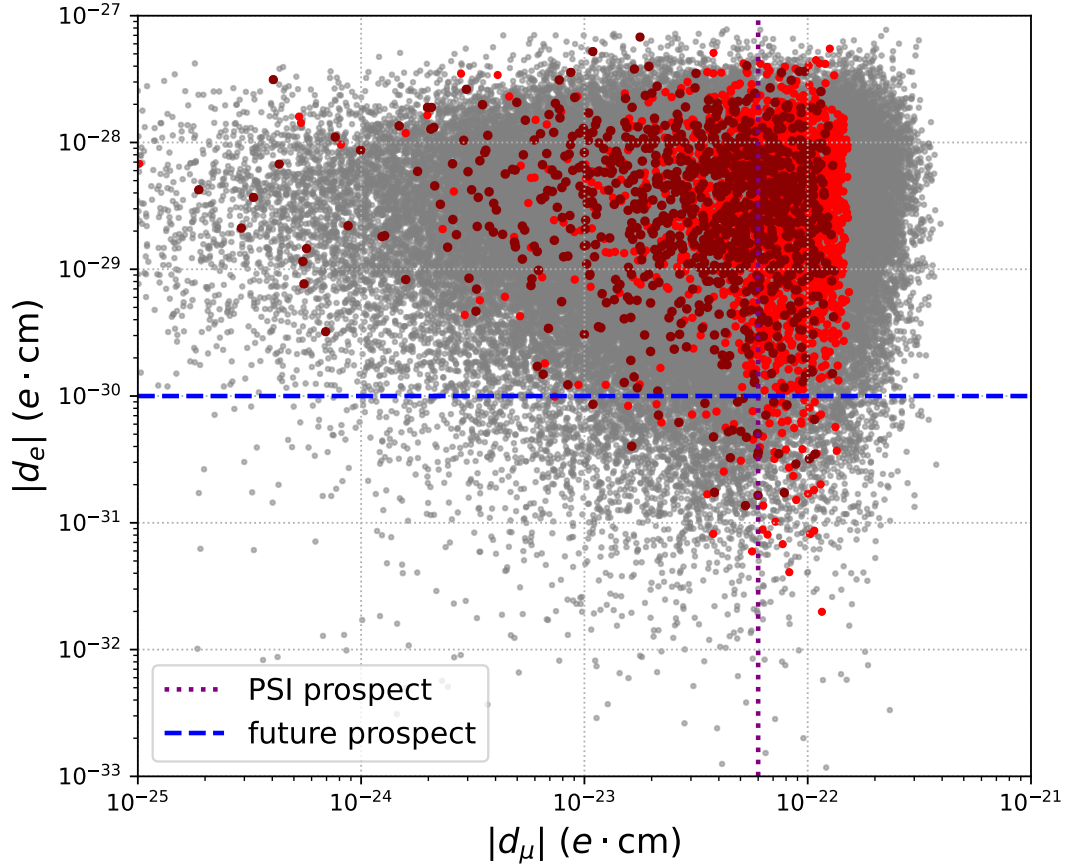


Figure 5: The correlations between the muon and electron EDMs. The gray dots show the points excluded by the $h \rightarrow \mu^+ \mu^-$ constraint. The (dark) red dots represent the points satisfying the (1σ) 2σ region of the muon $g - 2$. The blue band is the constraint from the ACME experiment for the electron EDM measurement. The prospect of the PSI experiment for the muon EDM measurement and the near-future electron EDM experiments are shown as the vertical dotted line and horizontal dashed line, respectively.

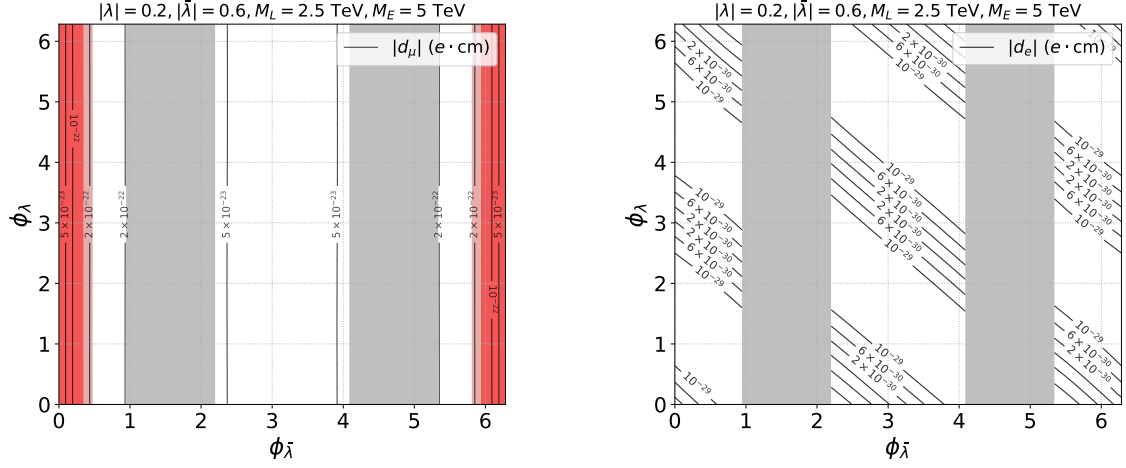


Figure 6: The dependence of muon EDM (left) and electron EDM (right) on the two CP -violating phases in the model. The other parameters are chosen to be $|\lambda| = 0.2$, $|\bar{\lambda}| = 0.6$, $M_E = 2.5 \text{ TeV}$, $M_L = 5 \text{ TeV}$, $\lambda_L = -0.04 \times \sqrt{2}M_L/v \sim -0.57$, and $\lambda_E = 0.03 \times \sqrt{2}M_E/v \sim 0.86$. The size of the EDMs are given by the black contours. The gray bands represent the regions where no solution exists for the y_μ to give the correct muon mass after the mass diagonalization. The region consistent with muon $g - 2$ at (2σ) 1σ level is also indicated in the left figure by the (light) red bands.

violating phases, $\phi_{\bar{\lambda}}$ and ϕ_λ , in Fig. 6. Here, we fix the other parameters to be $|\lambda| = 0.2$, $|\bar{\lambda}| = 0.6$, $M_E = 2.5 \text{ TeV}$, $M_L = 5 \text{ TeV}$, $\lambda_L = -0.04 \times \sqrt{2}M_L/v \sim -0.57$, and $\lambda_E = 0.03 \times \sqrt{2}M_E/v \sim 0.86$. The magnitude of the EDMs is indicated by the black contours. The gray bands are the regions where no solution exists for the y_μ to give the correct muon mass after the mass diagonalization. The (2σ) 1σ level of muon $g - 2$ are also given in the left figure as the (light) red bands. As we can see from the plots, the muon EDM only depends on one of the two CP -violating phases, $\phi_{\bar{\lambda}}$, while in the case of the electron EDM, it depends on both of the phases. If the muon EDM is indeed nonzero and the vector-like leptons exist, we may be able to determine the masses and couplings of the vector-like leptons from the measurement of their decays, and the value of $\phi_{\bar{\lambda}}$ can then be fixed by the result of the muon EDM measurement. We can input these parameters to the electron EDM and find the value of the remaining phase ϕ_λ according to the result of the electron EDM measurement.

7 Summary

In this work, we have investigated a simple extension of the Standard Model, with the addition of one $SU(2)_L$ doublet and one $SU(2)_L$ singlet vector-like leptons, which are coupled to the second-generation SM leptons only. In this framework, the muon dipole moments are generated through the mediation of the Higgs, W , and Z bosons. Furthermore, one interesting feature of this model is that a sizable electron EDM can also be induced at the two-loop level. Besides the latest value of the muon $g - 2$ published by the Muon $g - 2$ collaboration at the Fermilab, we have also considered the recent constraint on the Higgs decay channel $h \rightarrow \mu^+\mu^-$ reported by the CMS group and the constraint on

the electron EDM from the ACME experiment. We have found that there are parameter regions consistent with all these constraints.

Because of the chirality flip from the heavy vector-like leptons, the sizes of muon dipole moments are enhanced. The muon EDM can be as large as $10^{-22} e \cdot \text{cm}$, which can be probed in the future muon EDM measurement such as the PSI experiment, whose sensitivity is estimated to be around $6 \times 10^{-23} e \cdot \text{cm}$ [10]. An electron EDM of $\mathcal{O}(10^{-30}) e \cdot \text{cm}$ can be generated in this model, and future electron EDM measurement like the ACME III experiment, whose sensitivity is expected to be one order of magnitude better than the previous ACME II [55], is able to examine the prediction.

Acknowledgments

This work is supported in part by the Grant-in-Aid for Innovative Areas (No.19H05810 [KH], No.19H05802 [KH], No.18H05542 [NN]), Scientific Research B (No.20H01897 [KH and NN]), Young Scientists (No.21K13916 [NN]), and JSPS KAKENHI Grant (No.20J22214 [SYT]).

A Interactions

In this appendix, we briefly summarize the interactions in the model we used in the analysis. Concerning the index notation, the quantities related to the flavor basis are indexed by Greek alphabets ($\alpha, \beta, \gamma, \dots$), while the quantities related to the mass basis are indexed by Latin alphabets (i, j, k, \dots). For the flavor indices, we have $2 = \mu, 4 = L$ and $5 = E$.

A.1 Higgs boson couplings

Since the couplings related to electron and tau are not modified by the vector-like leptons, their couplings with the Higgs boson are the SM values $\lambda_{e,\tau} = -m_{e,\tau}/v$. Other couplings of charged leptons to the Higgs boson are modified by the mixings. The Yukawa interaction in the flavor basis is given by

$$\mathcal{L}_Y \supset -\frac{1}{\sqrt{2}} \bar{f}_{L\rho} Y_{\rho\sigma} f_{R\sigma} h + \text{h.c.} \quad (38)$$

This can be transformed to the mass basis given by

$$\mathcal{L}_Y \supset -\frac{1}{\sqrt{2}} \sum_{\rho,\sigma=2,4,5} \bar{f}_{Li} (U_L^\dagger)_{i\rho} Y_{\rho\sigma} (U_R)_{\sigma j} f_{Rj} h + \text{h.c.} \equiv \bar{f}_{Li} \lambda_{ij} f_{Rj} h + \text{h.c.}, \quad (39)$$

where the Yukawa matrix is written as

$$Y = \begin{pmatrix} y_\mu & 0 & \lambda_E \\ \lambda_L & 0 & \lambda \\ 0 & \bar{\lambda} & 0 \end{pmatrix}, \quad (40)$$

and the Yukawa couplings in the mass basis is

$$\lambda_{ij} = -\frac{1}{\sqrt{2}} \sum_{\rho, \sigma=2,4,5} (U_L^\dagger)_{i\rho} Y_{\rho\sigma} (U_R)_{\sigma j}. \quad (41)$$

We notice that the Yukawa coupling in the flavor basis is similar to the mass matrix of the charged leptons with the absence of the masses of vector-like leptons, that is, $Yv/\sqrt{2} = M - \text{diag}(0, M_L, M_E)$. With this relation, the Higgs boson couplings in the mass basis can be written as:

$$-\lambda v = U_L^\dagger \begin{pmatrix} y_\mu v/\sqrt{2} & 0 & \lambda_E v/\sqrt{2} \\ \lambda_L v/\sqrt{2} & M_L & \lambda v/\sqrt{2} \\ 0 & \bar{\lambda} v/\sqrt{2} & M_E \end{pmatrix} U_R - U_L^\dagger \begin{pmatrix} 0 & 0 & 0 \\ 0 & M_L & 0 \\ 0 & 0 & M_E \end{pmatrix} U_R \quad (42)$$

$$= \begin{pmatrix} m_\mu & 0 & 0 \\ 0 & m_4 & 0 \\ 0 & 0 & m_5 \end{pmatrix} - U_L^\dagger \begin{pmatrix} 0 & 0 & 0 \\ 0 & M_L & 0 \\ 0 & 0 & M_E \end{pmatrix} U_R. \quad (43)$$

In this expression, we can see clearly that the first term has a simple form which is the same as the Yukawa couplings in the SM. The second term corresponds solely to the contributions from the mass term of the vector-like leptons.

A.2 Z boson couplings

The couplings of leptons to the Z boson come from the kinetic term of the leptons. Due to the mixing among muon and vector-like leptons, the kinetic term is modified to

$$\mathcal{L}_{\text{kin}} \supset \bar{f}_{L\sigma} i \not{D}_\sigma f_{L\sigma} + \bar{f}_{R\sigma} i \not{D}_\sigma f_{R\sigma} = \bar{f}_{Li} (U_L^\dagger)_{i\sigma} i \not{D}_\sigma (U_L)_{\sigma j} f_{Lj} + \bar{f}_{Ri} (U_R^\dagger)_{i\sigma} i \not{D}_\sigma (U_R)_{\sigma j} f_{Rj}. \quad (44)$$

The covariant derivative $D_{\mu\sigma}$ is defined as

$$D_{\mu\sigma} = \partial_\mu + i \frac{g}{\cos \theta_W} (T_\sigma^3 - Q_\sigma \sin^2 \theta_W) Z_\mu + ie Q_\sigma A_\mu, \quad (45)$$

where e and g are the electromagnetic and the SU(2) couplings of the Standard Model, and T^3 and Q are the weak isospin and electric charge of leptons obtained from the quantum numbers listed in Table 1.

The couplings of the Z boson to charged leptons ℓ_i and ℓ_j are defined in the Lagrangian

$$\mathcal{L}_Z \supset [\bar{f}_{Li} \gamma^\mu (g_L^Z)_{ij} f_{Lj} + \bar{f}_{Ri} \gamma^\mu (g_R^Z)_{ij} f_{Rj}] Z_\mu. \quad (46)$$

The couplings of left-handed and right-handed charged leptons with Z boson are given by

$$(g_L^Z)_{ij} = -\frac{g}{\cos \theta_W} \sum_{\sigma=2,4,5} (T_{L\sigma}^3 - \sin^2 \theta_W Q_\sigma) (U_L^\dagger)_{i\sigma} (U_L)_{\sigma j}, \quad (47)$$

$$(g_R^Z)_{ij} = -\frac{g}{\cos \theta_W} \sum_{\sigma=2,4,5} (T_{R\sigma}^3 - \sin^2 \theta_W Q_\sigma) (U_R^\dagger)_{i\sigma} (U_R)_{\sigma j}, \quad (48)$$

Flavor	2	4	5
Q_σ	-1	-1	-1
$T_{L\sigma}^3$	-1/2	-1/2	0
$T_{R\sigma}^3$	0	-1/2	0

Table 3: This table shows the electric charge Q_σ and the third component of weak isospins $T_{L\sigma}^3$ and $T_{R\sigma}^3$ for each flavor considered in the mixing of charged leptons. Recall that in the flavor basis, we have $2 = \mu$, $4 = L$, and $5 = E$.

where the electric charge Q_σ and the third component of weak isospins $T_{L\sigma}^3$ and $T_{R\sigma}^3$ for each flavor are summarized in Table 3.

Since the electric charge Q_σ is the same for all the charged leptons considered, no modification is made on the couplings of photon with charged leptons. On the other hand, because of the different weak isospins of the charged leptons in the mixing, the couplings of the Z boson in Eq. (47) and Eq. (48) are modified from their SM values. In $(g_L^Z)_{ij}$, we have

$$-\frac{g}{\cos\theta_W} \left\{ \left(-\frac{1}{2} + \sin^2\theta_W \right) [(U_L^\dagger)_{i2}(U_L)_{2j} + (U_L^\dagger)_{i4}(U_L)_{4j}] + \sin^2\theta_W (U_L^\dagger)_{i5}(U_L)_{5j} \right\}. \quad (49)$$

To see the modification to the SM coupling, we can arrange and separate Eq. (47) in two parts. The first one is

$$-\frac{g}{\cos\theta_W} \left\{ \left(-\frac{1}{2} + \sin^2\theta_W \right) [(U_L^\dagger)_{i2}(U_L)_{2j} + (U_L^\dagger)_{i4}(U_L)_{4j} + (U_L^\dagger)_{i5}(U_L)_{5j}] \right\}. \quad (50)$$

By the unitarity of the matrix U_L , we have $\sum_{\sigma=2,4,5} (U_L^\dagger)_{i\sigma}(U_L)_{\sigma j} = \delta_{ij}$. This gives the form of the SM coupling of Z boson with the left-handed leptons

$$(g_L^Z)_{ij}^{\text{SM}} = -\frac{g}{\cos\theta_W} \left(-\frac{1}{2} + \sin^2\theta_W \right) \delta_{ij}. \quad (51)$$

The second one corresponds to the modification of the SM coupling,

$$(\delta g_L^Z)_{ij} = -\frac{g}{2\cos\theta_W} (U_L^\dagger)_{i5}(U_L)_{5j}. \quad (52)$$

Similarly, we can separate Eq. (48) in parts of the SM coupling

$$(g_R^Z)_{ij}^{\text{SM}} = -\frac{g}{\cos\theta_W} \sin^2\theta_W \delta_{ij} \quad (53)$$

and the modification

$$(\delta g_R^Z)_{ij} = \frac{g}{2\cos\theta_W} (U_R^\dagger)_{i4}(U_R)_{4j}. \quad (54)$$

A.3 W boson couplings

The couplings of W with leptons are also derived from the kinetic term. Since the charged lepton E is an $SU(2)_L$ singlet, it decouples from the interaction with W boson. The kinetic term is given by

$$\mathcal{L}_{\text{kin}} \supset -\frac{g}{\sqrt{2}} \left(\bar{\nu}_\mu \gamma^\mu \mu_L + \bar{L}_L^0 \gamma^\mu L_L^- + \bar{L}_R^0 \gamma^\mu L_R^- \right) W_\mu^+ + h.c. \quad (55)$$

$$= -\frac{g}{\sqrt{2}} \left(\bar{\nu}_2 \gamma^\mu (U_L)_{2j} f_{Lj} + \bar{\nu}_{L4} \gamma^\mu (U_L)_{4j} f_{Lj} + \bar{\nu}_{R4} \gamma^\mu (U_R)_{4j} f_{Rj} \right) W_\mu^+ + h.c.. \quad (56)$$

This can be written in a more compact form

$$\mathcal{L}_W \supset \left[\bar{\nu}_{Li} \gamma^\mu (g_L^W)_{ij} f_{Lj} + \bar{\nu}_{Ri} \gamma^\mu (g_R^W)_{ij} f_{Rj} \right] W_\mu^+ + h.c., \quad (57)$$

and the couplings of W boson with leptons are defined as

$$(g_L^W)_{2j} = -\frac{g}{\sqrt{2}} (U_L)_{2j}, \quad (g_L^W)_{4j} = -\frac{g}{\sqrt{2}} (U_L)_{4j}, \quad (g_R^W)_{4j} = -\frac{g}{\sqrt{2}} (U_R)_{4j}, \quad (58)$$

with $(g_R^W)_{2j} = (g_L^W)_{5j} = (g_R^W)_{5j} = 0$.

A.4 Couplings in the electron EDM formulas

The interaction of the Higgs boson with the charged leptons is

$$\bar{f}_{Li} \lambda_{ij} f_{Rj} h + \bar{f}_{Ri} \lambda_{ji}^* f_{Lj} h = \bar{f}_i (\lambda_{ij} P_R + \lambda_{ji}^* P_L) f_j h, \quad (59)$$

where $P_{L,R}$ are the projection operators for the left-handed and right-handed components of the leptons. This can be rearranged in the form of the scalar and pseudoscalar couplings

$$\bar{f}_i (g_s^{ij} + g_p^{ij} \gamma_5) f_j h, \quad (60)$$

where

$$g_s^{ij} = \frac{1}{2} (\lambda_{ij} + \lambda_{ji}^*), \quad g_p^{ij} = \frac{1}{2} (\lambda_{ij} - \lambda_{ji}^*) \quad (61)$$

are the scalar and pseudoscalar types of coupling.

The interaction of charged leptons with Z boson can be written as

$$\bar{f}_i \gamma^\mu \left(g_v^{Z,ij} + g_a^{Z,ij} \gamma_5 \right) f_j Z_\mu, \quad (62)$$

where

$$g_v^{Z,ij} = \frac{1}{2} \left[(g_L^Z)_{ij} + (g_R^Z)_{ij} \right], \quad g_a^{Z,ij} = \frac{1}{2} \left[(-g_L^Z)_{ij} + (g_R^Z)_{ij} \right] \quad (63)$$

are the vector and axial-vector types of coupling.

The electron couplings in Eq. (29) are given by

$$g_s^{ee} = -m_e/v, \quad (64)$$

$$g_v^{\gamma ee} = e, \quad (65)$$

$$g_v^{Zee} = -\frac{g}{4 \cos \theta_W} \left(-1 + 4 \sin^2 \theta_W \right), \quad g_a^{Zee} = -\frac{g}{4 \cos \theta_W}. \quad (66)$$

	e	μ	τ	H	$L_{L,R}$	$E_{L,R}$	σ	σ'	N_e	N_μ	N_τ
$U(1)_{L_\mu-L_\tau}$	0	1	-1	0	1	1	1	0	0	1	-1
$U(1)_{B+3L_e-L_\mu-5L_\tau}$	3	-1	-5	0	-1	-1	2	6	3	-1	-5

Table 4: Charge assignment of gauged $U(1)_{L_\mu-L_\tau}$ and $U(1)_{B+3L_e-L_\mu-5L_\tau}$ symmetries to the fields considered in the model in appendix B.

B An example for the muon-only coupling

In the model discussed in our work, we just assume that the vector-like leptons couple only to the second-generation leptons, not to the first- and third-generation ones. In this appendix, we briefly discuss a model where this setup is realized as a consequence of $U(1)$ gauge symmetries.

As discussed in Refs. [57, 58], there are two types of lepton flavor-dependent $U(1)$ symmetries which can be gauged and introduced to a model without anomalies. One is the linear combination of the lepton numbers $U(1)_{\alpha_e L_e + \alpha_\mu L_\mu - (\alpha_e + \alpha_\mu) L_\tau}$ and the other is a linear combination of baryon and lepton numbers $U(1)_{B + \beta_e L_e + \beta_\mu L_\mu - (3 + \beta_e + \beta_\mu) L_\tau}$. As an example, we choose them to be $U(1)_{L_\mu-L_\tau}$ and $U(1)_{B+3L_e-L_\mu-5L_\tau}$. The charge assignment of the fields is summarized in Table 4. Note that we introduce three right-handed neutrinos, N_e, N_μ, N_τ . To break the new $U(1)$ gauge symmetries, we also introduce two scalar fields that are singlet under the SM gauge interactions, σ and σ' . We choose the charges of the vector-like leptons to be the same as the ones of muon so that the interaction structure of coupling solely to the muon in Eq. (8) can be realized. The charges of the new scalars are chosen for the reason explained in the following.

After the spontaneous symmetry breaking of scalar fields, we obtain a Majorana mass matrix of the right-handed neutrinos in the form of

$$\begin{pmatrix} \lambda_{ee}\langle\sigma'^*\rangle & \lambda_{e\mu}\langle\sigma^*\rangle & \lambda_{e\tau}\langle\sigma\rangle \\ \lambda_{e\mu}\langle\sigma^*\rangle & 0 & \lambda_{\mu\tau}\langle\sigma'\rangle \\ \lambda_{e\tau}\langle\sigma\rangle & \lambda_{\mu\tau}\langle\sigma'\rangle & 0 \end{pmatrix}, \quad (67)$$

while the neutrino Dirac mass matrix is diagonal. This implies that after applying the seesaw mechanism [59–62], we obtain an active neutrino mass matrix with the so-called two-zero minor structure [63, 64]. We can then follow the same analysis performed in [65–67] to extract the predictions of the sum of three active neutrino masses and the Dirac CP -violating phase δ .

In Fig. 7, we show these predictions as a function of the neutrino mixing angle θ_{23} , with other two mixing angles and the two squared mass differences fixed by the values provided in [68]. The neutrino masses are taken to be in the normal ordering, $m_1 < m_2 < m_3$, as the inverse ordering turns out to be incompatible with the observed neutrino oscillation data in this model [65]. In both plots, the boundary of x axis corresponds to the 3σ range of θ_{23} , while the vertical dashed line shows the central value of θ_{23} and the 1σ range of θ_{23} are enclosed by the vertical dotted lines. The horizon dashed line in the left plot represents the upper bound on the sum of active neutrino masses given in [69], which is $\sum m_\nu < 0.13$ eV at 95% confidence level. The (light) green band in the right plot shows the

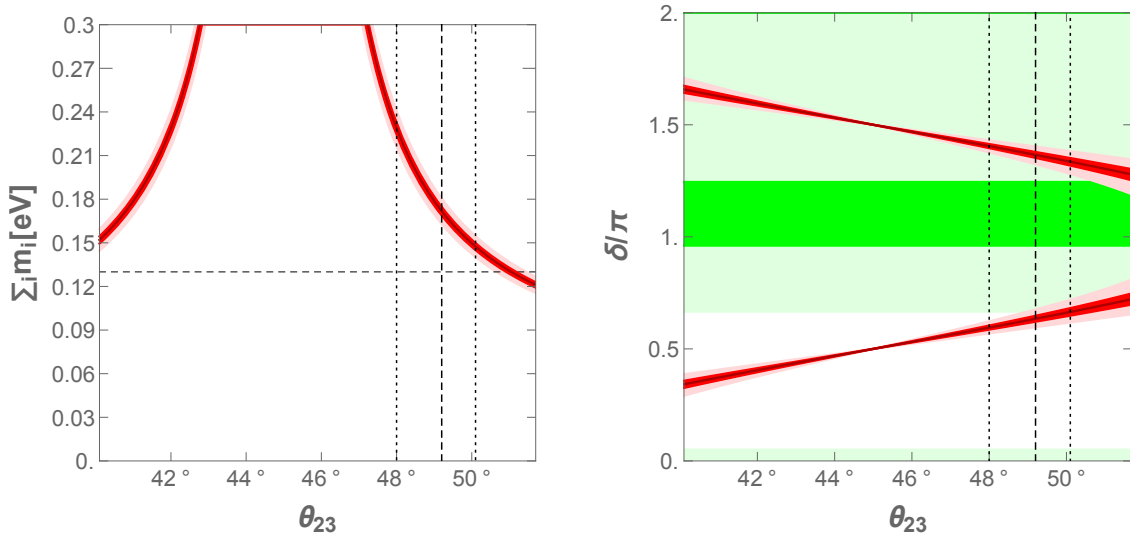


Figure 7: Left plot: predictions of the sum of the three active neutrino masses as a function of θ_{23} . Right plot: predictions of the Dirac CP phase as a function of θ_{23} . The predictions are plotted as red curves, dark (light) red bands corresponding to the parameters fixed to their central value and 1 (3) sigma value given in [68]. In both plots, the boundary of x axis corresponds to the 3σ range of θ_{23} , while the vertical dashed line shows the central value of θ_{23} and the 1σ range of θ_{23} are enclosed by the vertical dotted lines. The horizon dashed line in the left plot represents the upper bound on the sum of the active neutrino masses given in [69], which is $\Sigma m_\nu < 0.13$ eV at 95% confidence level. The (light) green band in the right plot shows the (3) 1σ range of the Dirac CP -violating phase obtained in [68].

(3) 1σ range of the Dirac CP -violating phase obtained in [68]. The predictions from the two-zero minor structure are plotted as red curves, dark (light) red bands corresponding to the parameters fixed to their central value and 1 (3) sigma value, respectively, given in [68]. As we can see from the plots, although a large fraction of the parameter region are excluded by the constraint on the sum of the neutrino masses, there is still a possibility around the corner close to the 3σ boundary of θ_{23} , which can be examined in the future neutrino experiments.

References

- [1] **Muon g-2** Collaboration, *Measurement of the Positive Muon Anomalous Magnetic Moment to 0.46 ppm*, *Phys. Rev. Lett.* **126** (2021) 141801 [[arXiv:2104.03281](#)].
- [2] T. Aoyama *et al.*, *The anomalous magnetic moment of the muon in the Standard Model*, *Phys. Rept.* **887** (2020) 1–166 [[arXiv:2006.04822](#)].
- [3] S. Borsanyi *et al.*, *Leading hadronic contribution to the muon magnetic moment from lattice QCD*, *Nature* **593** (2021) 51–55 [[arXiv:2002.12347](#)].

- [4] M. Cè *et al.*, *Window observable for the hadronic vacuum polarization contribution to the muon $g - 2$ from lattice QCD*, [arXiv:2206.06582](#) (2022).
- [5] C. Alexandrou *et al.*, *Lattice calculation of the short and intermediate time-distance hadronic vacuum polarization contributions to the muon magnetic moment using twisted-mass fermions*, [arXiv:2206.15084](#) (2022).
- [6] M. Pospelov and A. Ritz, *Electric dipole moments as probes of new physics*, *Annals Phys.* **318** (2005) 119–169 [[hep-ph/0504231](#)].
- [7] **Muon (g-2)** Collaboration, *An Improved Limit on the Muon Electric Dipole Moment*, *Phys. Rev. D* **80** (2009) 052008 [[arXiv:0811.1207](#)].
- [8] **ACME** Collaboration, *Improved limit on the electric dipole moment of the electron*, *Nature* **562** (2018) 355–360.
- [9] M. Abe *et al.*, *A New Approach for Measuring the Muon Anomalous Magnetic Moment and Electric Dipole Moment*, *PTEP* **2019** (2019) 053C02 [[arXiv:1901.03047](#)].
- [10] A. Adelmann *et al.*, *Search for a muon EDM using the frozen-spin technique*, [arXiv:2102.08838](#) (2021).
- [11] K. Kannike, M. Raidal, D. M. Straub, and A. Strumia, *Anthropic solution to the magnetic muon anomaly: the charged see-saw*, *JHEP* **02** (2012) 106 [[arXiv:1111.2551](#)]. [Erratum: *JHEP* 10, 136 (2012)].
- [12] A. Falkowski, D. M. Straub, and A. Vicente, *Vector-like leptons: Higgs decays and collider phenomenology*, *JHEP* **05** (2014) 092 [[arXiv:1312.5329](#)].
- [13] R. Dermisek and A. Raval, *Explanation of the Muon $g-2$ Anomaly with Vectorlike Leptons and its Implications for Higgs Decays*, *Phys. Rev. D* **88** (2013) 013017 [[arXiv:1305.3522](#)].
- [14] P. Arnan, L. Hofer, F. Mescia, and A. Crivellin, *Loop effects of heavy new scalars and fermions in $b \rightarrow s\mu^+\mu^-$* , *JHEP* **04** (2017) 043 [[arXiv:1608.07832](#)].
- [15] E. Megias, M. Quiros, and L. Salas, *$g_\mu - 2$ from Vector-Like Leptons in Warped Space*, *JHEP* **05** (2017) 016 [[arXiv:1701.05072](#)].
- [16] K. Kowalska and E. M. Sessolo, *Expectations for the muon $g-2$ in simplified models with dark matter*, *JHEP* **09** (2017) 112 [[arXiv:1707.00753](#)].
- [17] S. Raby and A. Trautner, *Vectorlike chiral fourth family to explain muon anomalies*, *Phys. Rev. D* **97** (2018) 095006 [[arXiv:1712.09360](#)].
- [18] Z. Poh and S. Raby, *Vectorlike leptons: Muon $g-2$ anomaly, lepton flavor violation, Higgs boson decays, and lepton nonuniversality*, *Phys. Rev. D* **96** (2017) 015032 [[arXiv:1705.07007](#)].
- [19] J. Kawamura, S. Raby, and A. Trautner, *Complete vectorlike fourth family and new $U(1)'$ for muon anomalies*, *Phys. Rev. D* **100** (2019) 055030 [[arXiv:1906.11297](#)].

- [20] G. Hiller, C. Hormigos-Feliu, D. F. Litim, and T. Steudtner, *Anomalous magnetic moments from asymptotic safety*, *Phys. Rev. D* **102** (2020) 071901 [[arXiv:1910.14062](#)].
- [21] G. Hiller, C. Hormigos-Feliu, D. F. Litim, and T. Steudtner, *Model Building from Asymptotic Safety with Higgs and Flavor Portals*, *Phys. Rev. D* **102** (2020) 095023 [[arXiv:2008.08606](#)].
- [22] M. Endo and S. Mishima, *Muon $g - 2$ and CKM unitarity in extra lepton models*, *JHEP* **08** (2020) 004 [[arXiv:2005.03933](#)].
- [23] M. Frank and I. Saha, *Muon anomalous magnetic moment in two-Higgs-doublet models with vectorlike leptons*, *Phys. Rev. D* **102** (2020) 115034 [[arXiv:2008.11909](#)].
- [24] E. J. Chun and T. Mondal, *Explaining $g - 2$ anomalies in two Higgs doublet model with vector-like leptons*, *JHEP* **11** (2020) 077 [[arXiv:2009.08314](#)].
- [25] K. Kowalska and E. M. Sessolo, *Minimal models for $g-2$ and dark matter confront asymptotic safety*, *Phys. Rev. D* **103** (2021) 115032 [[arXiv:2012.15200](#)].
- [26] R. Dermisek, K. Hermanek, and N. McGinnis, *Muon $g-2$ in two-Higgs-doublet models with vectorlike leptons*, *Phys. Rev. D* **104** (2021) 055033 [[arXiv:2103.05645](#)].
- [27] H. M. Lee and K. Yamashita, *A model of vector-like leptons for the muon $g - 2$ and the W boson mass*, *Eur. Phys. J. C* **82** (2022) 661 [[arXiv:2204.05024](#)].
- [28] A. de Giorgi, L. Merlo, and S. Pokorski, *The Low-Scale Seesaw Solution to the M_W and $(g - 2)_\mu$ Anomalies*, [arXiv:2211.03797](#) (2022).
- [29] K. S. Babu, B. Dutta, and R. N. Mohapatra, *Enhanced electric dipole moment of the muon in the presence of large neutrino mixing*, *Phys. Rev. Lett.* **85** (2000) 5064–5067 [[hep-ph/0006329](#)].
- [30] T. Ibrahim and P. Nath, *Slepton flavor nonuniversality, the muon EDM and its proposed sensitive search at Brookhaven*, *Phys. Rev. D* **64** (2001) 093002 [[hep-ph/0105025](#)].
- [31] J. L. Feng, K. T. Matchev, and Y. Shadmi, *Theoretical expectations for the muon’s electric dipole moment*, *Nucl. Phys. B* **613** (2001) 366–381 [[hep-ph/0107182](#)].
- [32] A. Romanino and A. Strumia, *Electron and Muon Electric Dipoles in Supersymmetric Scenarios*, *Nucl. Phys. B* **622** (2002) 73–94 [[hep-ph/0108275](#)].
- [33] J. R. Ellis, J. Hisano, S. Lola, and M. Raidal, *CP violation in the minimal supersymmetric seesaw model*, *Nucl. Phys. B* **621** (2002) 208–234 [[hep-ph/0109125](#)].
- [34] J. R. Ellis, J. Hisano, M. Raidal, and Y. Shimizu, *Lepton electric dipole moments in nondegenerate supersymmetric seesaw models*, *Phys. Lett. B* **528** (2002) 86–96 [[hep-ph/0111324](#)].

- [35] A. Bartl, W. Majerotto, W. Porod, and D. Wyler, *Effect of supersymmetric phases on lepton dipole moments and rare lepton decays*, *Phys. Rev. D* **68** (2003) 053005 [[hep-ph/0306050](#)].
- [36] K. Cheung, O. C. W. Kong, and J. S. Lee, *Electric and anomalous magnetic dipole moments of the muon in the MSSM*, *JHEP* **06** (2009) 020 [[arXiv:0904.4352](#)].
- [37] G. Hiller, K. Huitu, T. Ruppell, and J. Laamanen, *A Large Muon Electric Dipole Moment from Flavor?*, *Phys. Rev. D* **82** (2010) 093015 [[arXiv:1008.5091](#)].
- [38] C. Cesarotti, Q. Lu, Y. Nakai, A. Parikh, and M. Reece, *Interpreting the Electron EDM Constraint*, *JHEP* **05** (2019) 059 [[arXiv:1810.07736](#)].
- [39] W. Dekens, J. de Vries, M. Jung, and K. K. Vos, *The phenomenology of electric dipole moments in models of scalar leptoquarks*, *JHEP* **01** (2019) 069 [[arXiv:1809.09114](#)].
- [40] A. Crivellin, M. Hoferichter, and P. Schmidt-Wellenburg, *Combined explanations of $(g-2)_{\mu,e}$ and implications for a large muon EDM*, *Phys. Rev. D* **98** (2018) 113002 [[arXiv:1807.11484](#)].
- [41] W. Altmannshofer, S. Gori, H. H. Patel, S. Profumo, and D. Tuckler, *Electric dipole moments in a leptoquark scenario for the B -physics anomalies*, *JHEP* **05** (2020) 069 [[arXiv:2002.01400](#)].
- [42] I. Bigaran and R. R. Volkas, *Reflecting on chirality: CP -violating extensions of the single scalar-leptoquark solutions for the $(g-2)_{e,\mu}$ puzzles and their implications for lepton EDMs*, *Phys. Rev. D* **105** (2022) 015002 [[arXiv:2110.03707](#)].
- [43] Y. Omura, E. Senaha, and K. Tobe, *τ - and μ -physics in a general two Higgs doublet model with $\mu - \tau$ flavor violation*, *Phys. Rev. D* **94** (2016) 055019 [[arXiv:1511.08880](#)].
- [44] W.-S. Hou, G. Kumar, and S. Teunissen, *Charged lepton EDM with extra Yukawa couplings*, *JHEP* **01** (2022) 092 [[arXiv:2109.08936](#)].
- [45] Y. Nakai, R. Sato, and Y. Shigekami, *Muon electric dipole moment as a probe of flavor-diagonal CP violation*, *Phys. Lett. B* **831** (2022) 137194 [[arXiv:2204.03183](#)].
- [46] R. Dermisek, K. Hermanek, N. McGinnis, and S. Yoon, *Ellipse of Muon Dipole Moments*, *Phys. Rev. Lett.* **129** (2022) 221801 [[arXiv:2205.14243](#)].
- [47] Y. Ema, T. Gao, and M. Pospelov, *Improved Indirect Limits on Muon Electric Dipole Moment*, *Phys. Rev. Lett.* **128** (2022) 131803 [[arXiv:2108.05398](#)].
- [48] S. M. Barr and A. Zee, *Electric Dipole Moment of the Electron and of the Neutron*, *Phys. Rev. Lett.* **65** (1990) 21–24. [Erratum: *Phys. Rev. Lett.* **65**, 2920 (1990)].
- [49] Y. Nakai and M. Reece, *Electric Dipole Moments in Natural Supersymmetry*, *JHEP* **08** (2017) 031 [[arXiv:1612.08090](#)].

- [50] **CMS Collaboration**, *Evidence for Higgs boson decay to a pair of muons*, **JHEP** **01** (2021) 148 [[arXiv:2009.04363](#)].
- [51] **LHC Higgs Cross Section Working Group Collaboration**, *Handbook of LHC Higgs Cross Sections: 4. Deciphering the Nature of the Higgs Sector*, [arXiv:1610.07922](#) (2016).
- [52] **Particle Data Group Collaboration**, *Review of Particle Physics*,. to be published (2022).
- [53] **L3 Collaboration**, *Search for heavy neutral and charged leptons in e^+e^- annihilation at LEP*, **Phys. Lett. B** **517** (2001) 75–85 [[hep-ex/0107015](#)].
- [54] **CMS Collaboration**, *Inclusive nonresonant multilepton probes of new phenomena at $\sqrt{s}=13$ TeV*, **Phys. Rev. D** **105** (2022) 112007 [[arXiv:2202.08676](#)].
- [55] *The ACME EDM Experiment*, <http://doylegroup.harvard.edu/edm/>.
- [56] R. Alarcon *et al.* in *2022 Snowmass Summer Study*. 2022. [arXiv:2203.08103](#).
- [57] T. Araki, J. Heeck, and J. Kubo, *Vanishing Minors in the Neutrino Mass Matrix from Abelian Gauge Symmetries*, **JHEP** **07** (2012) 083 [[arXiv:1203.4951](#)].
- [58] K. Asai, *Predictions for the neutrino parameters in the minimal model extended by linear combination of $U(1)_{L_e-L_\mu}$, $U(1)_{L_\mu-L_\tau}$ and $U(1)_{B-L}$ gauge symmetries*, **Eur. Phys. J. C** **80** (2020) 76 [[arXiv:1907.04042](#)].
- [59] P. Minkowski, *$\mu \rightarrow e\gamma$ at a Rate of One Out of 10^9 Muon Decays?*, **Phys. Lett. B** **67** (1977) 421–428.
- [60] T. Yanagida, *Horizontal Symmetry and Masses of Neutrinos*, **Prog. Theor. Phys.** **64** (1980) 1103.
- [61] M. Gell-Mann, P. Ramond, and R. Slansky, *Complex Spinors and Unified Theories*, **Conf. Proc. C** **790927** (1979) 315–321 [[arXiv:1306.4669](#)].
- [62] R. N. Mohapatra and G. Senjanovic, *Neutrino Mass and Spontaneous Parity Nonconservation*, **Phys. Rev. Lett.** **44** (1980) 912.
- [63] L. Lavoura, *Zeros of the inverted neutrino mass matrix*, **Phys. Lett. B** **609** (2005) 317–322 [[hep-ph/0411232](#)].
- [64] E. I. Lashin and N. Chamoun, *Zero minors of the neutrino mass matrix*, **Phys. Rev. D** **78** (2008) 073002 [[arXiv:0708.2423](#)].
- [65] K. Asai, K. Hamaguchi, and N. Nagata, *Predictions for the neutrino parameters in the minimal gauged $U(1)_{L_\mu-L_\tau}$ model*, **Eur. Phys. J. C** **77** (2017) 763 [[arXiv:1705.00419](#)].
- [66] K. Asai, K. Hamaguchi, N. Nagata, S.-Y. Tseng, and K. Tsumura, *Minimal Gauged $U(1)_{L_\alpha-L_\beta}$ Models Driven into a Corner*, **Phys. Rev. D** **99** (2019) 055029 [[arXiv:1811.07571](#)].

- [67] K. Asai, K. Hamaguchi, N. Nagata, and S.-Y. Tseng, *Leptogenesis in the minimal gauged $U(1)_{L_\mu-L_\tau}$ model and the sign of the cosmological baryon asymmetry*, **JCAP** **11** (2020) 013 [[arXiv:2005.01039](#)].
- [68] I. Esteban, M. C. Gonzalez-Garcia, M. Maltoni, T. Schwetz, and A. Zhou, *The fate of hints: updated global analysis of three-flavor neutrino oscillations*, **JHEP** **09** (2020) 178 [[arXiv:2007.14792](#)].
- [69] **DES** Collaboration, *Dark Energy Survey Year 3 results: Cosmological constraints from galaxy clustering and weak lensing*, **Phys. Rev. D** **105** (2022) 023520 [[arXiv:2105.13549](#)].